Fabrication of pH-Responsive Nanocomposites of Gold Nanoparticles/Poly(4-vinylpyridine)

Dongxiang Li,[†] Qiang He,[†,‡] Yue Cui,[†] and Junbai Li*,[†]

Beijing National Laboratory for Molecular Sciences (BNLMS), International Joint Lab, CAS Key Lab of Colloid and Interface Science, Institute of Chemistry, Chinese Academy of Sciences, Zhong Guan Cun, Beijing 100080, People's Republic of China, and Max Planck Institute of Colloids and Interfaces, 14476 Golm/Potsdam, Germany

Received September 25, 2006. Revised Manuscript Received December 6, 2006

Novel nanocomposites of gold nanoparticle and poly(4-vinylpyridine) (Au@PVP) were fabricated through surface-initiated atom-transfer radical polymerization (SI-ATRP) at ambient conditions. The citrate-stabilized gold nanoparticles were first modified by a disulfide initiator for ATRP initiation, and the following polymerization of 4-vinylpyridine (4VP) occurred on the surface of gold particles. The assembled Au@PVP nanocomposites are pH-responsive because of the pyridyl groups, which are facially protonated and positively charged. At low pH (<3.2), the polymer chains attached on gold nanoparticles are expanded by electrostatic forces, and the polymer layer is loosely swelled; hence, the Au@PVP composite particle displays a comatulid-like nanostructure in 3-D AFM images. However, at a relatively high pH (>3.2), the polymer chains shrink and wrap around the gold particle surface, which results in the aggregation of gold nanoparticles with a thin shrunken polymer layer under TEM observation. Such assembled Au@PVP nanocomposites as a smart supporter can entrap transition metal ions by their efficient coordinating segments, and subsequently, the metal ions can be reduced in situ to construct novel bimetallic nanocomposites, which are regarded as intelligent catalysts with environmental stimuli activity.

Introduction

Metal nanoparticles have attracted continuous interest owing to their unusual properties and potential uses in electronics, optics, magnetics, catalysts, and sensors.[1−6] As a well-known noble metal, gold is widely investigated due to its specific impact in the fields of biotechnology and bioscience.[7−10] A large number of polymer molecules have been selected to decorate the surface of gold nanoparticles in physical or chemical manners for different purposes.[11−16] The surface-initiated atom-transfer radical polymerization (SI-ATRP) is becoming a popular method to construct a core−shell structure on the particle surface.[17−22] Poly(4-vinylpyridine) (PVP) as a water soluble polymer and coordinative reagent for transition metals has been paid much attention in recent years.[23−25] It is often used to extract heavy metals in waste water treatment[26,27] and also as a host ligand of metal-containing chromophores.[28,29] Moreover, the pH-sensitive PVP polymer can be readily quaternized by alkylogen and subsequently form the positively charged

* Corresponding author. Tel.: +86 10 82614087. Fax: +86 10 82612629. E-mail: jbli@iccas.ac.cn.
[†] Chinese Academy of Sciences.
[‡] Max Planck Institute of Colloids and Interfaces.

(1) Hostetler, M. J.; Zhong, C. J.; Yen, B. K. H.; Anderegg, J.; Gross, S. M.; Evans, N. D.; Porter, M.; Murray, R. W. *J. Am. Chem. Soc.* **1998**, *120*, 9396.
(2) Liu, S.; Zhang, Z.; Han, M. *Adv. Mater.* **2005**, *17*, 1862.
(3) Zhu, H. F.; Tao, C.; Zheng, S. P.; Li, J. B. *Colloids Surf., A* **2005**, *257*, 411.
(4) Bastys, V.; Pastoriza-Santos, I.; Rodríguez-González, B.; Vaisnoras, R.; Liz-Marzán, L. M. *Adv. Funct. Mater.* **2006**, *16*, 766.
(5) Zhu, H. F.; Tao, C.; Zheng, S. P.; Wu, S. K.; Li, J. B. *Colloids Surf., A* **2005**, *256*, 17.
(6) Dong, H.; Fey, E.; Gandelman, A.; Jones, W. E. *Chem. Mater.* **2006**, *18*, 2008.
(7) Neimeyer, C. M. *Angew. Chem., Int. Ed.* **2001**, *40*, 4128.
(8) Daniel, M. C.; Astruc, D. *Chem. Rev.* **2004**, *104*, 293.
(9) Brayner, R.; Coradin, T.; Vaulay, M.-J.; Mangeney, C.; Livage, J.; Fiévet, F. *Colloids Surf., A* **2005**, *256*, 191.
(10) Fan, H.; Wright, A.; Gabaldon, J.; Rodriguez, A.; Brinker, C. J.; Jiang, Y. B. *Adv. Funct. Mater.* **2006**, *16*, 891.
(11) Wuelfing, W. P.; Gross, S. M.; Miles, D. T.; Murray, R. W. *J. Am. Chem. Soc.* **1998**, *120*, 12696.
(12) Teranishi, T.; Kiyokawa, I.; Miyake, M. *Adv. Mater.* **1998**, *10*, 596.
(13) Lowe, A. B.; Sumerlin, B. S.; Donovan, M. S.; McCormick, C. L. *J. Am. Chem. Soc.* **2002**, *124*, 11562.
(14) Jordan, R.; West, N.; Ulman, A.; Chou, Y.; Nuyken, O. *Macromolecules* **2001**, *34*, 1606.
(15) Watson, K. J.; Zhu, J.; Nguyen, S. T.; Mirkin, C. A. *J. Am. Chem. Soc.* **1999**, *121*, 462.
(16) Raula, J.; Shan, J.; Nuopponen, M.; Niskanen, A.; Jiang, H.; Kauppinen, E. I.; Tenhu, H. *Langmuir* **2003**, *19*, 3499.
(17) Patten, T. E.; Matyjaszewski, K. *Adv. Mater.* **1998**, *10*, 901.
(18) Nuss, S.; Böttcher, H.; Wurm, H.; Hallensleben, M. L. *Angew. Chem., Int. Ed.* **2001**, *40*, 4016.
(19) Ohno, K.; Koh, K.; Tsujii, Y.; Fukuda, T. *Macromolecules* **2002**, *35*, 8989.
(20) Mandal, T. K.; Fleming, M. S.; Walt, D. R. *Nano Lett.* **2002**, *2*, 3.
(21) Duan, H.; Kuang, M.; Zhang, G.; Wang, D.; Kurth, D. G.; Möhwald, H. *Langmuir* **2005**, *21*, 11495.
(22) Duan, H.; Kuang, M.; Wang, D.; Kurth, D. G.; Möhwald, H. *Angew. Chem., Int. Ed.* **2005**, *44*, 1717.
(23) Fischer, A.; Brembilla, A.; Lochon, P. *Macromolecules* **1999**, *32*, 6069.
(24) Bohrisch, J.; Wendler, U.; Jaeger, W. *Macromol. Rapid Commun.* **1997**, *18*, 975.
(25) Harnish, B.; Robinson, J. T.; Pei, Z.; Ramström, O.; Yan, M. *Chem. Mater.* **2005**, *17*, 4092.
(26) Rivas, B. L.; Quilodran, B.; Quiroz, E. *J. Appl. Polym. Sci.* **2004**, *92*, 2908.
(27) El-Hamshary, H.; El-Garawany, M.; Assubaie, F. N.; Al-Eed, M. *J. Appl. Polym. Sci.* **2003**, *89*, 2522.
(28) Caruso, U.; Centore, R.; Panunzi, B.; Roviello, A.; Tuzi, A. *Eur. J. Inorg. Chem.* **2005**, 2747.
(29) Caruso, U.; Maria, A. D.; Panunzi, B.; Roviello, A. *J. Polym. Sci., Part A: Polym. Chem.* **2002**, *40*, 2987.

10.1021/cm062290+ CCC: $37.00
Published on Web 01/13/2007

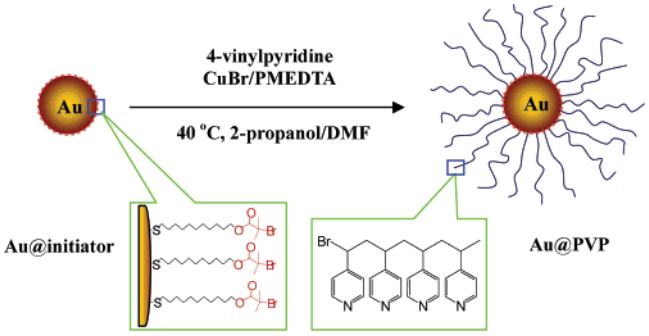

Figure 1. Schematic fabrication of Au@PVP nanoparticles by SI-ATRP.

polyelectrolytes as sensors and actuators[30,31] and the N-alkylated pyridinium polymers as antimicrobial materials.[32]

In this paper, we report the fabrication of PVP modified gold nanoparticles as pH-responsive nanocomposite materials by SI-ATRP on a gold surface. The typical experimental procedure is schematically illustrated in Figure 1. First, the disulfide initiator was immobilized on the surface of gold nanoparticles (Au@initiator). Subsequently, ATRP of 4-vinylpyridine (4VP) occurred on gold nanoparticles catalyzed by *N*,*N*,*N*′,*N*′,*N*″-pentamethyldiethylenetriamine (PMDETA) and CuBr. The obtained Au@PVP nanocomposites are pH responsive at a critical point of pH 3.2 revealed by surface plasmon resonance (SPR) changes of gold nanoparticles. Such environmentally responsive nanocomposites with effective coordinating pyridyl segments provide a smart supporter or carrier to transition metal ions and nanoparticles to construct novel bimetallic nanocomposites, especially in catalyst applications.

Experimental Procedures

Materials. 11-Mercapto-1-undecanol, 2-bromo-2-methylpropionyl bromide, 4VP, and PMDETA were purchased from Sigma-Aldrich. CuBr, $HAuCl_4$, H_2PtCl_6, sodium citrate, and other chemicals were obtained from Beijing Chemical Reagent Co., Beijing, China. 4VP was purified to remove the inhibitor. The disulfide initiator $[S\text{-}(CH_2)_{11}\text{-}OCOC(CH_3)_2Br]_2$ for ATRP was synthesized from 11-mercapto-1-undecanol and 2-bromo-2-methylpropionyl bromide through a modified procedure according to ref 33. The gold nanoparticles with an average diameter of 20 nm were prepared from $HAuCl_4$ and sodium citrate by conventional citrate-reduction methods.[34]

Preparation of SI-ATRP Initiator. The initiator immobilized on gold nanoparticles (Au@initiator) was prepared from fresh gold nanoparticles through ligand exchange between disulfide initiator and citrates. Generally, a certain volume of fresh gold nanoparticles in water was slowly added to same volume of a *N*,*N*-dimethylformamide (DMF) solution that dissolved 3.0 mM initiator with stirring for 24 h. The Au@initiator was collected and washed with DMF and Millipore purified deionized water by centrifugation. Finally, Au@initiator was dispersed in DMF and stored at −20 °C under an argon atmosphere.

SI-ATRP Process of 4VP. Polymerization of 4VP on a gold surface was performed in a mixed solvent at ambient conditions according to the literature.[35−38] In detail, a round-bottom flask was added with CuBr (28.6 mg) and degassed by three freeze−pump−thaw cycles under N_2 atmosphere. A degassed mixture of Au@initiator (2 mg) dissolved in DMF (2 mL), PMDETA (0.208 mL), 2-propanol (0.5 mL), and a certain amount of free initiator (0.5−20 mg) was injected into the flask through a syringe, followed by degassed 4VP (1.05−2.10 g) with drastic stirring. The reaction was performed for 24 h at 40 °C and terminated by opening the system to air. The Au@PVP nanocomposites were purified by more than three cycles of centrifugation, 2-propanol/DMF washing. The supernate in centrifugation was dialyzed with a pH 1.2 HCl solution to remove the monomer and catalyst. The obtained solution of free polymer was precipitated with 0.1 M NaOH, and the deposition was separated and dissolved in methanol followed by reduction with sodium borohydride to break the possible disulfide bond. Then, the solvent methanol was evaporated, and the aqueous phase was discarded. The resultant precipitate was washed by deionized water and dried in vacuum for molecular weight measurements.

pH Response of Au@PVP Nanocomposites. The Au@PVP nanocomposites were dispersed in HCl solutions at pH 1.2−5.6 and water at pH 7.4, respectively. Then, the samples were treated by ultrasonication several times and incubated for 2 days to reach equilibrium. The UV−vis spectra were then recorded from 800 to 200 nm, and the SPR response data were collected. Furthermore, the pH-response properties of these samples in different pH solutions were dropped on carbon-coated copper grids for transmission electron microscope (TEM) observations and also adsorbed on a new cleaved mica surface for atomic force microscope (AFM) measurements.

Nanocomplex of Au@PVP and Platinum. The coordinated complex of Au@PVP nanocomposites and platinum was prepared by adding H_2PtCl_6 (0.2 mL, 1.0 mg/mL) into Au@PVP nanoparticles (2 mL, 0.1 nM) in a pH 2.1 HCl solution, followed by continuous stirring for 24 h. The red loose precipitate was redispersed by ultrasonication and washed by a pH 2.1 HCl solution three times by centrifugation. Second, the platinum ions attached on the redispersed Au@PVP nanocomposites were reduced by a sodium borohydride solution with drastic stirring,[39] and then the mixture was centrifuged to separate and purify the composite bimetal nanoparticles.

Instrumentation. FT−IR and UV−vis spectra, respectively, were recorded on a TENSOR 27 instrument (BRUCKER) and a U-3010 UV−vis spectrometer (HITACHI). AFM measurements were performed on NanoScope IIIa (Veeco, Woodbury, NY) using tapping mode. TEM images were obtained by a TECNAI 20 transition electron microscope (PHILIPS), and the energy dispersive X-ray microanalysis (EDX) result was gained on a PHOENIX Microanalysis instrument. X-ray photoelectron spectroscopy (XPS) was performed on an ESCALab220i-XL electron spectrometer (VG Scientific) using 300 W Al Kα radiation at about 3×10^{-9} mbar, and the binding energies were referenced to the C1s line at 284.8 eV from adventitious carbon.

(30) Li, Y.; Yang, M.; She, Y. *Sens. Actuators, B* **2005**, *107*, 252.
(31) Aydogdu, Y.; Erol, I.; Yakuphanoğlu, F.; Aydogu, A.; Ahmedzade, M. *Synth. Met.* **2003**, *139*, 327.
(32) Tiller, J. C.; Lee, S. B.; Lewis, K.; Klibanov, A. M. *Biotechnol. Bioeng.* **2002**, *79*, 465.
(33) Shah, R. R.; Merreceyes, D.; Husemann, M.; Rees, I.; Abbott, N. L.; Hawker, C. J.; Hedrick, J. L. *Macromolecules* **2000**, *33*, 597.
(34) Link, S.; El-Sayed, M. A. *J. Phys. Chem. B* **1999**, *103*, 8410.
(35) Hao, E.; Lian, T. *Langmuir* **2000**, *16*, 7879.
(36) Ruokolainen, J.; Brinke, G.; Ikkala, O.; Torkkeli, M.; Serimaa, R. *Macromolecules* **1996**, *29*, 3409.
(37) Cui, Y.; Tao, C.; Zheng, S. P.; He, Q.; Ai, S. F.; Li, J. B. *Macromol. Rapid Commun.* **2005**, *26*, 1552.
(38) Cui, Y.; Tao, C.; Tian, Y.; He, Q.; Li, J. B. *Langmuir* **2006**, *22*, 8205.
(39) Mei, Y.; Sharma, G.; Lu, Y.; Ballauff, M.; Drechsler, M.; Irrgang, T.; Kempe, R. *Langmuir* **2005**, *21*, 12229.

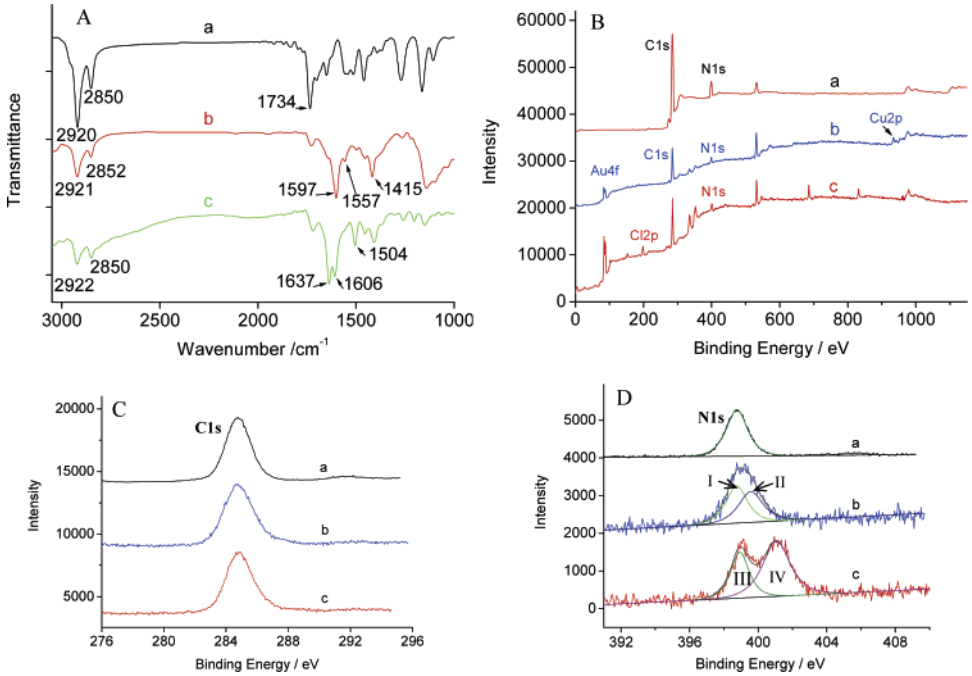

Figure 2. (A) FT−IR spectra of Au@initiator (a) and Au@PVP nanocomposites washed by 2-propanol (b) and treated with pH 1.2 HCl solution (c). (B) XPS survey profiles, (C) C1s spectra, and (D) N1s peak fitting of pure PVP (a) and Au@PVP nanocomposites before (b) and after (c) being treated with pH 2.1 HCl solution.

Results and Discussion

Fabrication and Characterizations of the Target Nanocomposites. The ATRP reaction of 4VP from a free initiator or a macromolecular initiator was suggested to be carried out in a protic alcohol solvent.[40,41] Herein, the solvent is mixed protic 2-propanol with DMF according to the solubility of the Au@initiator and PVP chains. The concentration of the 4VP monomer was adjusted from 0.2 to 0.4 g/mL, and SI-ATRP was performed at 40 °C. A large amount of PMDETA was used to compete with the pyridine component to maintain the activity of the catalytic system, and an appreciate amount of free initiator was added into the reaction mixture to control the polymerization.[42] Figure 2A shows the FT−IR spectra of Au@initiator and as-prepared Au@PVP nanocomposites. The profile of the Au@initiator (curve a) is similar to that of the pure disulfide initiator, whose characteristic absorbance at 2922, 2850 (CH_2 stretching), and 1734 cm^{-1} (ester carbonyl stretching) of Au@initiator (curve a) denotes the presence of the ATRP initiator on gold nanoparticles. For obtained Au@PVP (curve b), the characteristic peaks at 1597, 1557, and 1415 cm^{-1} represent the pyridyl ring-stretching vibrations according to the references (see Supporting Information Figure S1).[35,36] It shows that the polymerization of 4VP is performed successfully. However, after the samples were treated with a pH 1.2 HCl solution, the three characteristic peaks in the FT−IR spectra (curve c) shifted to 1637, 1606, and 1504 cm^{-1}, respectively. It is known that when the pyridyl groups are protonated, the characteristic bands of pyridinium groups will shift to higher frequencies by approximately 30−40 cm^{-1}.[35,36] So, the FT−IR results reveal that the Au@PVP nanocomposites are easily protonated by hydrochloride.

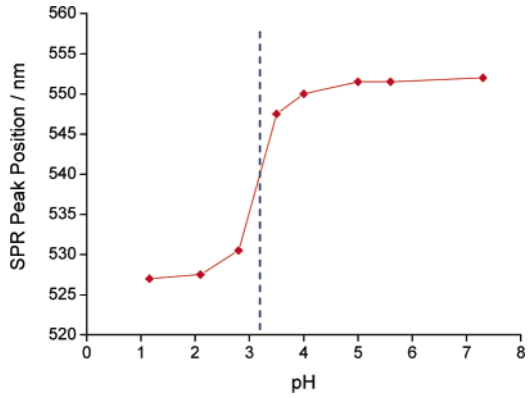

Figure 3. Au@PVP SPR peak position plot vs pH value. The SPR peak data were obtained from the analysis of UV−vis spectra at different pH values.

Moreover, the Au@PVP nanocomposite samples before and after treatment with the pH 2.1 HCl solution and pure PVP (sigma, as a comparison) were analyzed by X-ray photoelectron spectroscopy (XPS). The element components of Au@PVP nanocomposites are approximately contributed to C (69.6%), N (6.5%), S (1.2%), Au (2.1%), and Cu (1.9%), while the acidified samples are given the contributions of C (69.6%), N (7.7%), S (0.2%), Au (5.6%), and Cl (6.5%). The XPS survey profile of Au@PVP nanocomposites (curves b and c) in Figure 2B is similar to that of pure PVP (curve a). Figure 2C,D shows the peak details of the C1s and N1s spectra. It is found that these three C1s spectra display the same shape and indicate the circumstance consistency of carbon atoms. As shown in Figure 2D, the N1s peaks at 398.8 and 399.6 eV of Au@PVP (curve b) are contributed to one type of nitrogen atom (peak I) with the same binding energy to pure PVP (curve a) and an additional copper-coordinated nitrogen atoms (peak II). However, after the samples were acidified by the HCl solution, the binding energy of the typical nitrogen atoms (peak III) is similar to

(40) Xia, J.; Zhang, X.; Matyjaszawski, K. *Macromolecules* **1999**, *32*, 3531.
(41) Vidts, K. R. M.; Prez, F. E. D. *Eur. Polym. J.* **2006**, *42*, 43.
(42) Li, D. J.; Sheng, X.; Zhao, B. *J. Am. Chem. Soc.* **2005**, *127*, 6248.

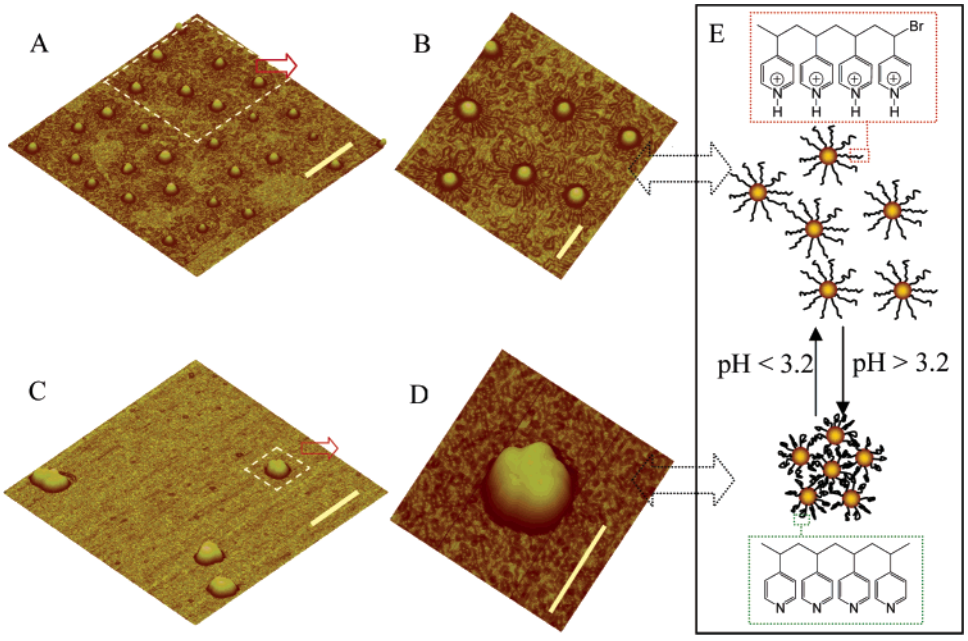

Figure 4. 3-D AFM images of Au@PVP nanoparticles (A), (B) at pH 1.2, and (C and D) at pH 5.0 with different magnifications. (E) Schematic mechanism illustration of pH response of Au@PVP nanocomposites. Scale bar: 500 nm in panels A and C and 200 nm in panels B and D.

that of pure PVP, and the other peak (peak IV) with a higher binding energy of 401.1 eV is attributed to the quarternized nitrogen atoms in pyridinium ions.[43] These results further verify the protonation of pyridyl groups under acidic conditions. In addition, considering that the sample has been purified carefully, the presence of copper in Au@PVP before acidification is ascribed to the coordination of a pyridyl segment. The Cu/N ratio is determined from XPS data as about 1:3.4. From the previous reports,[44−46] the coordination number of the copper ions was in the range of 1.5 to 4. As the coordination number is 1.5 with a maximum metal content, the amount of copper ions is excessive. In the case of the coordination number being 3.4, less than four pyridyl ligands are expected to bond.

The molecular weight and molecular weight distribution of grafted polymers formed on the surfaces are essentially identical to those of free polymers formed from free initiators in the system of SI-ATRP,[42,47−49] and such phenomena have been explained by the mechanism of the ATRP reaction.[50−52] The molecular weight and distribution of PVP were detected by gel permeation chromatography (GPC) (Figure S2A) using DMF as a solvent and eluent, and its composite was analyzed by ^{1}H NMR (Figure S2B). The number average molecular weight (M_n) is determined to be about 39 000 g/mol with a polydispersity index (M_w/M_n) of 1.33. This indicates that the polymer molecular weight has a relatively good distribution.

pH-Responsive Properties of Au@PVP Nanocomposites. Figure 3 shows the pH-stimuli SPR response of Au@PVP nanoparticles, which is collected from UV−vis spectra from pH 1.2 to 7.4. It is found that the SPR peak position changes from 551 nm at pH 7.4 to 526 nm at pH 1.2, and a rapid jump from pH 4.0 to 2.0 is exhibited with a critical point at pH 3.2. Such a pH-response curve can be fitted to a standard pH titration, and the apparent dissociation constant (pK_a) of Au@PVP nanocomposites is estimated at 3.2 with consistency to the result of the PVP membrane.[53] In addition, the pH response of these nanocomposites is reversible by the measurements of UV−vis spectra as in a previous report.[25]

In morphology, Figure 4 shows the 3-D AFM images of Au@PVP nanocomposites incubated at different pH environments. It can be seen that the composite nanoparticles have a good dispersity at pH 1.2 with a height of approximate 25.3 nm as shown in Figure 4A. The enlarged domain in Figure 4B displays typical comatulid-like nanostructures with many branches. The height of a single branch is about 1 nm by height section analysis on an AFM instrument, which is contributed to the polymer chains. As in the case of pH 5.0, Figure 4C shows the congeries of Au@PVP nanoparticles with an aggregating particle number of several to tens of numbers. Typically, Figure 4D shows a large aggregation of composite particles with a horizontal size of 150 nm and a height of 35.6 nm, which can be separated to six single nanoparticles on which the attached branches disappear. It denotes that the morphology of the Au@PVP nanocomposites is obviously altered as the pH value changes. To explain this, we propose a mechanism as shown in Figure 4E. The

(43) Cen, L.; Neoh, K. G.; Kang, E. T. *J. Biomed. Mater. Res.* **2004**, *71A*, 70.
(44) Kirsh, Y. E.; Kovner, V. Y.; Kokorin, A. I.; Zamaraev, K. I.; Chernyak, V. Y.; Kabanov, V. A. *Euro. Polym. J.* **1974**, *10*, 671.
(45) Jeschke, G. *J. Phys. Chem. B* **2000**, *104*, 8382.
(46) Agnew, N. H. *J. Polym. Sci., Polym. Chem. Ed.* **1976**, *14*, 2819.
(47) Husseman, M.; Malmström, E. E; McNamara, M.; Mate, M.; Mecerreyes, D.; Benoit, D. G.; Hedrick, J. L.; Mansky, P.; Huang, E.; Russell, T. P.; Hawker, C. J. *Macromolecules* **1999**, *32*, 1424.
(48) Bartholome, C.; Beyou, E.; Bourgeat-Lami, E.; Chaumont, P.; Zydowicz, N. *Macromolecules* **2003**, *36*, 7946.
(49) Ohno, K.; Morinaga, T.; Koh, K.; Tsujii, Y.; Fukuda, T. *Macromolecules* **2005**, *38*, 2137.
(50) Matyjaszawski, K.; Xia, J. H. *Chem. Rev.* **2001**, *101*, 2921.
(51) Sankhe, A. Y.; Husson, S. M.; Kilbey, S. M. *Macromolecules* **2006**, *39*, 1376.
(52) Braunecker, W. A.; Matyjaszawski, K. *J. Mol. Catal.* **2006**, *254*, 155.
(53) Mika, A. M.; Childs, R. F. *J. Membr. Sci.* **1999**, *152*, 129.

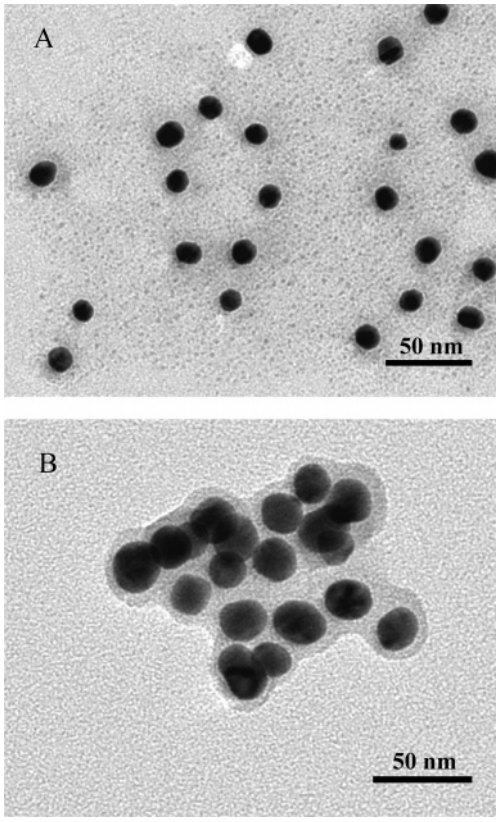

Figure 5. TEM images of Au@PVP nanocomposites (A) at pH 1.2 and (B) at pH 5.0, respectively.

pH response of Au@PVP nanoparticles is attributed to the protonation of a pyridyl segment into the pyridinium group, which leads to the polymer branches being positively charged.[35,36] In view of this, while the samples are incubated at a low pH (<3.2), the pyridyl ring will be protonated, so the positively charged polymer chains will repulse each other by the electrostatic interaction. This repulsive force will prevent the polymer coated particles from aggregation and also make polymer chains attached on same single particle expanded extensively. Therefore, the composite nanoparticles are monodispersed, and the attached polymer chains look like branches of comatulid as adsorbed on a mica surface. On the contrary, when the samples are incubated at a high pH (>3.2), the uncharged polymer chains will shrink and collapse onto the surface of core gold nanoparticles, and the simultaneous coiling of polymer chains results in a mass particle aggregation. However, the polymer layer on the gold surface will limit such aggregation to a certain degree; hence, the SPR peak shifts to a constant wavelength of about 550 nm. Alternatively, gold nanoparticles could also be coordinated to the nitrogen lone-pair electrons of adjacent PVP chains, which will also limit the expansion of polymer chains and may cause the aggregation as well.

Such a pH effect is also observed by the TEM measurements as shown in Figure 5. At pH 1.2, the gold particles as black cores are surrounded by the soft polymer layer as a grayish shell (Figure 5A), and these composite nanoparticles are well-dispersed, whereas at pH 5.0, the gold nanoparticle cores are enwrapped by the collapsed polymer chains with a distinct thin layer, and many gold particles are aggregated together (Figure 5B). Therefore, these morphological changes

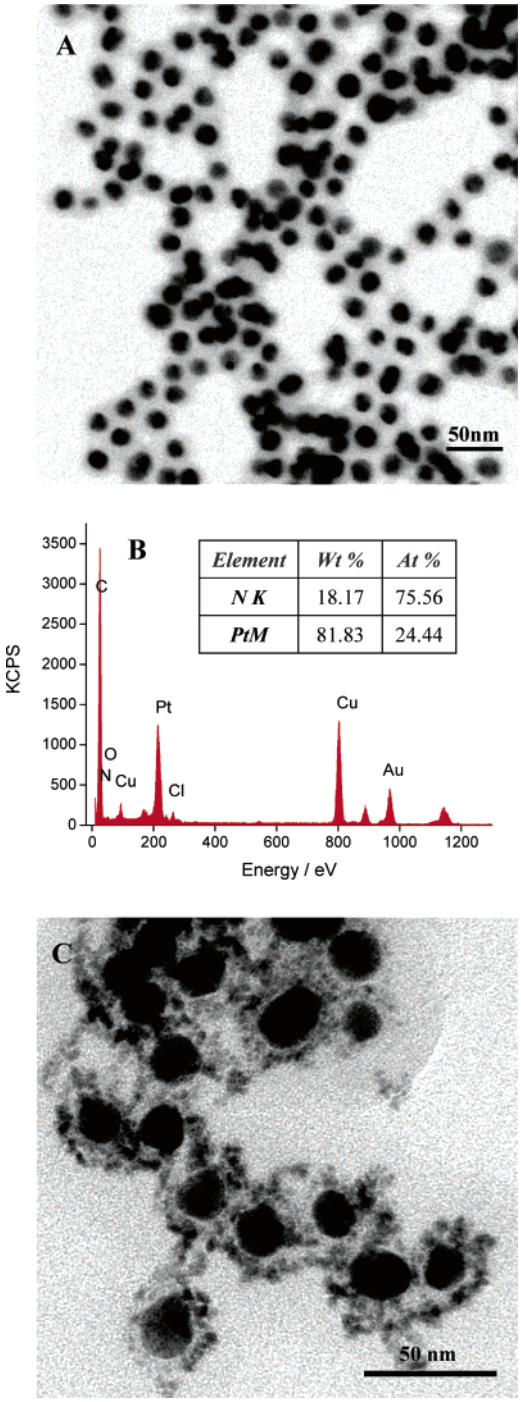

Figure 6. TEM image (A) and EDX spectrum (B) of coordinated complexes and bimetal nanocomposites (C) of the Au@PVP nanocomposites for the entrapment of platinum.

further demonstrate that the Au@PVP nanocomposite with a gold core and a peripheral polymer shell is assuredly pH responsive.

Potential Application as Supporters and Carriers. Such assembled Au@PVP nanoparticles can be considered as an effectively coordinating host to the ligand to entrap metal ions by means of pyridyl groups, which will provide an important basis for various applications.[45] Here, we employed chloroplatinic acid to obtain a coordinated complex and bimetal composites of Au@PVP nanoparticles and platinum. Figure 6A shows the TEM image of the complex purified by washing with pH 2.1 HCl solutions. It is found that the

Au@PVP nanoparticles are partially congregated because the adsorption of chloroplatinic anions on polymer chains results in charge neutralization. The EDX spectrum in Figure 6B provides evidence of the platinum existence with a Pt/N ratio of 1:3.1 (inset of Figure 6B). The platinum coordinates supported on gold nanoparticles can be regarded as a typical catalyst with high effectivity.[54,55] Furthermore, the coordinated platinum ions can be subsequently reduced in situ to metallic nanoparticles[39] as shown in Figure 6C. The platinum nanoparticles with a diameter of about 1−5 nm as a layer surround core gold nanoparticles, and such a core−shell nanostructure linked by an environmental stimuli polymer is regarded as a smart nanoreactor with modulating catalytic activity.[56] It is more interesting that the bimetallic gold−platinum catalyst composites can produce a welcome reduction of the cost of fuel cell installations in power sources.[57] Thus, the Au@PVP nanostructures as efficient supporters and carriers for transition metal ions or nanoparticles will exhibit significant importance in catalyst applications by means of the coordinate-active pyridine groups. In addition, we can predict that they can also directly entrap the negatively charged nanoparticles or biomolecules by their positively charged polymer shells at acidic conditions.

(54) Narayanan, R.; EI-Sayed, M. A. *J. Am. Chem. Soc.* **2003**, *125*, 8340.
(55) Li, C. F.; Li, D. X.; Feng, S. Y. *Polym. Int.* **2005**, *54*, 1041.
(56) Lu, Y.; Mei, Y.; Drechsler, M.; Ballauff, M. *Angew. Chem., Int. Ed.* **2006**, *45*, 813.
(57) Cameron, D.; Holliday, R.; Thompson, D. *J. Power Sources* **2003**, *118*, 298.

Conclusion

In summery, we have demonstrated that SI-ATRP of 4VP can be performed on the surface of initiator modified gold nanoparticles to fabricate pH-responsive gold−polymer nanocomposites. The as-prepared Au@PVP nanocomposites have a core−shell nanostructure with gold cores and polymer shells at a low pH, while at a high pH value, such Au@PVP particles will aggregate by the collapse of polymer layers. The composite nanoparticles have a reversible pH responsibility with a translation point at pH 3.2. Such Au@PVP nanocomposites as a smart supporter can entrap transition metal ions by their efficient coordinating segments, and subsequently, the metal ions can be reduced in situ to construct novel pH-stimuli bimetallic catalysts.

Acknowledgment. We acknowledge the financial support of this research by the National Nature Science Foundation of China (20471063, 20404015, 20403022, and 90206035), Chinese Academy of Sciences, and the collaborated project of the German Max Planck Society.

Supporting Information Available: Details of FT−IR spectra, ^{1}H NMR spectra, GPC profile, and UV−vis spectra at different pH. This material is available free of charge via the Internet at http://pubs.acs.org.

CM062290+